

A review on gold nanowire based SERS sensors for chemicals and biological molecules

Rashida Akter¹, Hyuck Jin Lee^{2,3}, Toeun Kim¹, Jin Woo Choi^{4,★}, and Hongki Kim^{1,3,★}

¹Department of Chemistry, Kongju National University, Gongju-si 32588, Korea

²Department of Chemistry Education, Kongju National University, Gongju-si 32588, Korea

³Earth Environment Research Center, Kongju National University, Gongju-si 32588, Korea

⁴Department of Data Information and Physics, Kongju National University, Gongju-si 32588, Korea

(Received May 8, 2024; Revised May 31, 2024; Accepted June 5, 2024)

Abstract: Surface-enhanced Raman scattering (SERS) has emerged as a powerful technique for detecting and analyzing chemical and biological molecules at ultra-low concentrations. The effectiveness of SERS largely depends on structures with sub-10 nm gaps, prompting the proposal of various nanostructures as efficient SERS-active platforms. Among these, single-crystalline gold nanowires (AuNWs) are particularly promising due to their large dielectric constants, well-defined geometries, atomically smooth surfaces, and surface plasmon resonance across the visible spectrum, which produce strong SERS enhancements. This review comprehensively explores the synthesis, functionalization, and application of Au NWs in SERS. We discuss various methods for synthesizing AuNWs, including the vapor transport method, which influences their morphological and optical properties. We also review practical applications in chemical and biosensing, showcasing the adaptability of Au NWs-based SERS platforms in detecting a range of analytes, from environmental pollutants to biological markers. The review concludes with a discussion on future perspectives that aim to enhance sensor performance and broaden application domains, highlighting the potential of these sensors to revolutionize diagnostics and environmental monitoring. This review underscores the transformative impact of AuNW-based SERS sensors in analytical chemistry, environmental science, and biomedical diagnostics, paving the way for next-generation sensing technologies.

Key words: surface enhanced raman spectroscopy, single-crystalline au nanowire, sensors

1. Introduction

Surface-enhanced Raman scattering (SERS) is a powerful method, where the light scattering by molecule is greatly enhanced when the molecules are adsorbed onto photonic nanostructures.¹ Thus, more detail

molecular and chemical information can be obtained from chemical and biological molecules in solution and/or at surfaces. Indeed, SERS is considered as a powerful analytical technique with ultrasensitive and fingerprint-diagnostic characteristics for molecule detection in the fields of analytical chemistry,

★ Corresponding author

Phone : +82-(0)41-850-8490 Fax : +82-(0)41-856-8613

E-mail : hongkikim@kongju.ac.kr

This is an open access article distributed under the terms of the Creative Commons Attribution Non-Commercial License (<http://creativecommons.org/licenses/by-nc/3.0>) which permits unrestricted non-commercial use, distribution, and reproduction in any medium, provided the original work is properly cited.

environmental science, and biomedical engineering.²

Due to its strong Raman signals enhancement at the metallic nanostructure, SERS has been widely used for the identification of chemical and biological species at trace levels such as nM and pM.³ The strong SERS signal enhancement permits the ultrasensitive detection of molecules even at the single molecule level.⁴ The remarkable SERS enhancement is mainly attributed to SERS hot spots, where the electric field becomes highly magnified when the incident light interacts with the small nm gaps of plasmonic nanostructures.^{5,6} The origin of SERS enhancement is described by two mechanisms; electromagnetic and chemical effects. The electromagnetic effect is based on the enhanced electromagnetic field at or near laser-irradiated noble metal particle surfaces as a result of localized surface plasmon resonance (LSPR).⁷ Most of normal SERS enhancements are caused by the electromagnetic enhancement.⁸ On the other hand, the chemical effect occurs from the specific interactions between analyte molecules and the metal nanoparticles.⁹ The chemical enhancement results from resonant charge transfer effects between a molecule, that is strongly chemically adsorbed onto the surface and the metal itself leading to 10^2 - 10^3 fold of the enhancement.⁹

Both electromagnetic and chemical enhancements strongly rely on the SERS substrate. The fabrication of highly reproducible and reliable SERS substrates is crucial for better understanding of SERS and its applications in chemical and biological molecules detection. The SERS substrates could be solid substrates or colloidal NPs dispersed solution. Both substrates have some merits. The colloidal NPs based substrates have advantages due to their cost-effective synthesis and the tailored optical properties by tuning particle size and shape.² On the other hand, solid substrates provides highly reproducible SERS signal and possibility for the large-scale production.

The SERS enhancement could be evaluated by the enhancement factor (EF), which is dominated by the gap-distance and surface density of hot spots.¹⁰ Generally, the EF is determined by the ratio of the detected Raman signals under SERS and normal conditions. The EF value is proportional to the fourth

power of the intensity of the local electromagnetic field ($|E|^4$), which results from both the incident and emitted photons enhancement.¹¹ The EF is also depends on both the SERS substrate and its fabrication method, which is typically in the range between 10^4 - 10^7 , although some SERS substrates exhibited high EFs range as 10^7 - 10^{14} .¹²⁻¹⁴ Importantly, nanoscale roughened surface is required for large SERS enhancements (high EF value) in both mechanisms, where the analyte is strongly adsorbed. Therefore, the selection of nanoscale SERS-active platform is a crucial for effective SERS enhancement. Various types of Au nanostructures based SERS-active platforms are developed which exhibit large SERS enhancement and are successfully used for biomolecules and chemical detection.¹⁵⁻¹⁹ The detections of organic dye molecules and pesticides are important as these molecules are widely used in various industries and in the agriculture fields. These toxic and health hazard chemical compounds could easily enter into human body through the intake of fish and agriculture products and can badly affect human health. On the other hand, detection of biological molecules has attracted increasing interest in clinical diagnostics and biomedical applications. For example, the detection of specific biological compounds as biomarkers in the disease diagnosis and monitoring is important and highly desirable. Thus, the SERS detection of these chemical and biological compounds need reproducible and stable SERS-active platform. Among various SERS platforms, gold nanowires (AuNWs) are superior to others because of their large dielectric constant and surface plasmon resonance in the entire visible range producing strong SERS enhancement.²⁰ Therefore, the fabrication of such AuNWs-based SERS-active platforms is greatly desirable for developing SERS chemical/biosensors for efficient chemical, biological and medical applications. Since AuNWs based SERS-active platforms can provide highly regular and reproducible SERS hot spots for the high sensitive and selective detection of an analyte of interest, thus, AuNWs are widely used in SERS detection of chemical and biological compounds.²¹⁻²⁷ Recently, a single AuNW based dual mode SERS/EC platforms has been reported for the sensitive

and selective detection of severe acute respiratory syndrome coronavirus-2 (SARS-CoV-2).²¹ Jia *et al.* has been developed a giant vesicles with tiny AuNWs-based SERS platform for the detection of a dye molecule, rhodamine 6G (R6G).²² A single AuNW-based SERS nanosensor has been reported for the detection of adenosine triphosphate (ATP).²³ A SERS platform based on straight upward AuNWs grown onto Fe₃O₄@TiO₂ matrix has been reported for the immunoassay detection of a colorectal and pancreatic cancer biomarker, cancer antigen 19-9 (CA19-9).²⁴ Another SERS-platform based on one-dimensional AuNWs supported silver aggregates for the immunoassay detection of a cancer biomarker prostate specific antigen (PSA) has been reported.²⁵ The vertical AuNWs-based SERS platform has been applied for the detection of ocular bacterial pathogens, *S. aureus*, *E. coli*, *P. aeruginosa*, and *S. epidermidis*.²⁶ Another interesting AuNWs forests based SERS-immunoassay kit for the detection of SARS-CoV-2 has been recently reported.²⁷ Although, various AuNWs-based SERS platforms have been recently widely used, however, the single-crystalline AuNWs-based SERS platform is more advantageous than conventional AuNWs due to the more SERS enhancement. Kang *et al.* reported a review on the synthesis of various single-crystalline AuNWs those could be used as SERS active platform; however, the sensing applications of those AuNWs have not been discussed.²⁸ Therefore, we summarize and discuss the advantages and potentials of the fabrications and applications of various single-crystalline AuNWs based SERS-sensors and biosensors in this review with two sections: (i) synthesis and fabrication of Au NWs and (ii) applications of AuNWs-based SERS platform in chemical and biosensing applications.

2. Synthesis and Fabrications of Au NWs

The AuNWs can be synthesized generally using nanotransfer printing and vapor transport methods, and solution based methods.^{10,29,30} Since the final products of AuNWs from solution based methods

showed relatively poor reproducibility of SERS signal due to the irregular distribution of the Au nanostructures during droplet evaporative self-assembly, the methods are not prefer way to prepare AuNWs. Therefore, the nanotransfer printing (nTP) and vapor transport methods will be discussed in this section. The nTP in particular solvent-assisted nTP (S-nTP) is a suitable method for controlling the 3D nanostructures.²⁹ The S-nTP technique is based on the fabrication of a master mold, the use of a polymer replica, metal deposition, and solvent-assisted debonding. Although, the excellent uniformity of Au NWs is a big advantages of nTP method, this method has disadvantages such as (i) complicated and composed of multi-steps fabrication process and (ii) use of various reagents and materials. On the other hand, the vapor transport (VT) method is simple, straight forward, and easy to use. Therefore, VT is widely employed for the synthesis of single-crystalline AuNWs.^{10,31-38}

Fig. 1(a) shows the schematic illustration of the preparation of AuNWs using VT method. In this method, Au precursor powder was put on an alumina boat. The sapphire substrate was placed a few centimeters downstream from the alumina boat. The temperature of the heating zone was brought to 1,100 °C and the pressure was maintained at 1-5 Torr. Ar gas flowed at a rate of 100 sccm was used to transport the Au vapor. The AuNWs were grown on the substrate and the synthesized AuNWs were single-crystalline having atomistically flat facets with diameters of 100–200 nm and length of up to tens of micrometers. The crossed and parallel AuNWs pairs were constructed by first synthesizing AuNWs through VT method and then transferring the AuNWs on a glass substrate with a nanomanipulator.¹⁰

A schematic illustration of the transferring process of the prepared AuNWs with a nanomanipulator is shown in *Fig. 1(b)*. Similarly, a single Au nanowire on an Au film (SNOF) was fabricated in which the single-crystalline Au NWs were first synthesized by using VT method and then incubated in analyte solution and finally casted on an Au film.⁶ The novel single Au nanowire on graphene (SNOG) structure was fabricated by firstly synthesizing Au NWs through

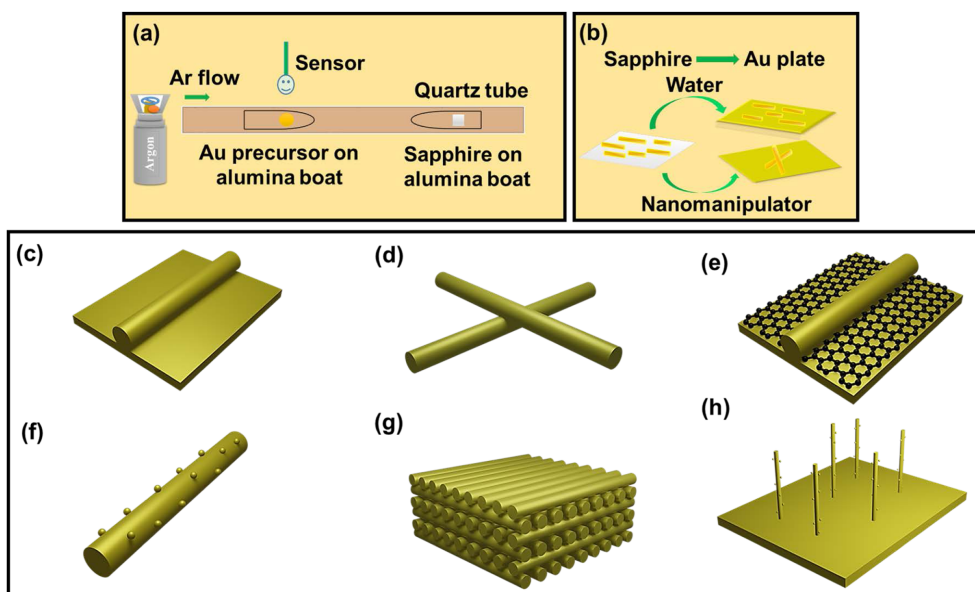


Fig. 1. (a) A schematic illustration of Au NWs preparation by VT method, (b) the prepared Au NWs transfer by water and nanomanipulator technique on various platforms for enhanced sensing, (c) a single Au NWs on a Au film (SNOF), (d) crossed Au NWs, (e) a single Au NW on graphene platform, (f) a Au NWs-Au NPs structure, (g) a 3D-cross-point nanostructure, and (h) free-standing Au NPs deposited Au NWs.

VT method on sapphire substrate and then transferred onto a monolayer graphene-coated metal film by using a simple attachment and detachment process.³⁵ For decorating the AuNWs with AuNPs (AuNWs/AuNPs), the nanogap-rich AuNWs were synthesized using VT method and AuNPs were deposited onto AuNWs by sputtering technique.³⁸ Additionally, AuNWs/AuNPs substrate was fabricated by firstly synthesized Au NWs by VT method on c-sapphire substrate and transferred onto a biotinylated Si substrate by custom-built nanomanipulator followed by immersing in PBS solution of avidin for 3 h (AuNWs/Bio/Avi).¹⁰ The AuNWs/Bio/Avi were incubated in biotinylated AuNPs solution for 3 h which formed AuNWs/AuNPs substrate.³¹ Schematic illustrations of the fabrications of various structured AuNWs based SERS platforms are shown in Fig. 1(c)-(h).

3. Applications of AuNWs Based SERS Platform in Chemical Sensing

SERS is widely recognized as a powerful ultrasensitive tool and AuNWs based SERS platforms have

been extensively employed in chemical sensing. However, practical application of SERS based sensor requires stable, reproducible, simple, and cheap fabrication process. In this section, the various single-crystalline AuNWs-based SERS chemicals sensor will be summarized.

Yoon *et al.* introduced a novel SERS-active platform based on SNOF for using as SERS chemical sensors and biosensor.⁶ The chemical structures and the corresponding SERS spectra for benzenethiol (BT), brilliant cresyl blue (BCB), and thiolated 10-mer

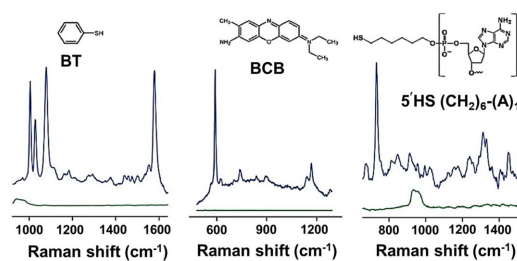


Fig. 2. Chemical structures and SERS spectra of BT, BCB, and HS-A10 for the Au/Au SNOF system (blue) and an Au NW on a Si substrate (green).⁶ Copyright 2009 American Chemical Society.

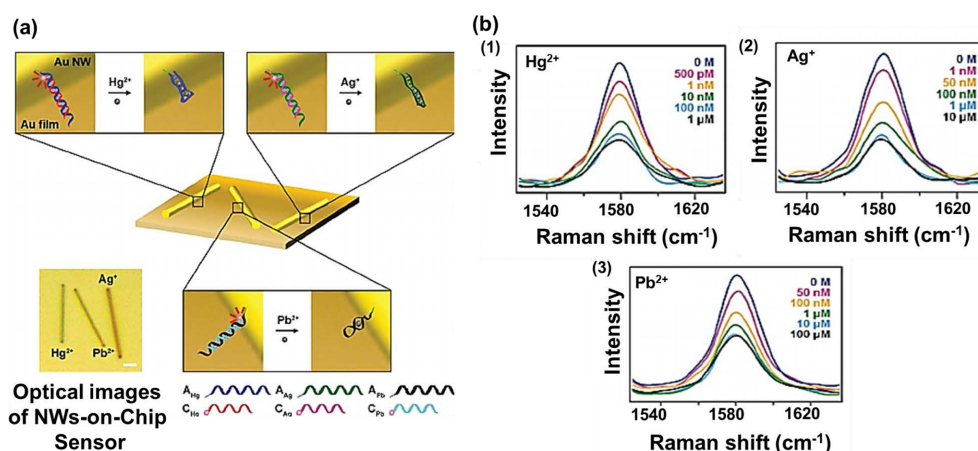


Fig. 3. (a) Schematic representation of the dsDNAs-modified single Au NWs on-chip sensor and (b) SERS spectra of cy5 at 1580 cm^{-1} obtained from the (1) Hg^{2+} , (2) Ag^+ , and (3) Pb^{2+} specific dsDNAs-modified NW-on-chip-sensor.²⁵ Reproduced with permission from Ref. 26. Copyright 2012, Royal Society of Chemistry.

adenine single-stranded DNA (HS-A10) using the Au/Au SNOF system (blue) and an AuNW on a Si substrate (green) are presented in Fig. 2. Single-crystalline AuNWs were used for fabricating SNOF platforms. The EF value of the platform was determined as 5.9×10^3 . The authors claimed that reproducible, stable and high sensitive SERS spectra could be observed for BT, BCB, and HS-A10. The other sensing parameters such as limit of detection (LOD) or relative standard deviation (RSD), however, were not presented.⁶

Jeong *et al.* reported the S-nTP method based AuNWs with 2D and 3D nanostructures and used to detect rhodamine 6G (R6G) molecules at 10^{-6} to 10^{-11} M concentration.²⁹ Average enhancement factor (AEF) values were obtained from the monolayer 2D AuNWs array and 3D AuNWs with vertically stacked up four layers as 5.2×10^3 and 4.9×10^4 , respectively. This high AEF of 3D AuNWs suggested that 3D AuNWs exhibited *ca.* 11 times higher signal enhancement than the 2D AuNWs array.²¹ The AuNWs/graphene hybrid nanostructure based SERS platform also showed 11-fold higher signal enhancement than the 2D AuNWs array without graphene.²¹ However, no reproducibility data for the 2D and 3D AuNWs based SERS platforms were reported, showing the S-nTP method of AuNWs based SERS platform has limitations for practical applications.²⁹

Kang *et al.* developed single-crystalline AuNWs-on-chip based SERS multiplex sensor for sensitive detection of multiple toxic metal ions.³³ Fig. 3 shows the schematic representation of the (i) Hg^{2+} (ii) Ag^+ , and (iii) Pb^{2+} specific dsDNAs-modified NW-on-chip sensor and SERS spectra of Cy5 at 1580 cm^{-1} obtained from the (i) Hg^{2+} (ii) Ag^+ , and (iii) Pb^{2+} specific dsDNAs-modified NW-on-chip sensor. The detachment of the reporter from the AuNWs-on-chip substrate in the present of metal ion resulted a decrease in the SERS signal. Thus, simple, rapid, sensitive, and quantitative detection of metal ions was possible by using the reporter. The detections of three metal ions were achieved through a single step using the reporter elimination method. Fig. 3(a) and 3(b) shows the schematic representation of the dsDNAs-modified single Au NWs on-chip sensor and SERS spectra of cy5 at 1580 cm^{-1} obtained from the (1) Hg^{2+} , (2) Ag^+ , and (3) Pb^{2+} , respectively. The substrate successfully detected Hg^{2+} , Ag^+ , and Pb^{2+} coexisting in the same solution with LODs of 500 pM, 1 nM, and 50 nM, respectively. Moreover, the AuNWs-on-chip sensors exhibited excellent reproducibility, making it suitable for real-time, onsite, and on-line detection of metal ions.³³ Kim *et al.* developed an efficient SERS-active platform based on a novel SNOG.³⁵ A single crystalline AuNW was assembled on a monolayer graphene-coated metal film. The SNOG substrate could

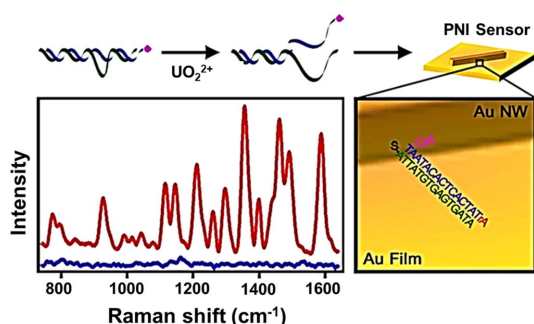


Fig. 4. Schematic illustration of UO_2^{2+} detection by a plasmonic nanowire (NW) interstice (PNI) sensor combined with a DNAzyme-cleaved reaction.²⁸ The left panel shows the SERS spectra measured from PNI sensors in the absence of (blue spectrum) and the presence of 10 nM UO_2^{2+} (red spectrum) and the right panel shows the modification of a PNI sensor.

provide extremely reproducible and stable SERS signals due to its continuous nanogap structure. The EF of the SNOG platform was calculated to be 1.18×10^6 , which was higher than that of AuNW on the Au film (7.36×10^5). This high EF of the SNOG platform might be related to the synergistic effects of electromagnetic enhancement of single-crystalline AuNWs and chemical enhancement of graphene. The RSD was determined to be 6.17 %, indicating high reproducibility of the SNOG platform.³⁵

Gwak *et al.* developed a plasmonic nanowire interstice (PNI) sensor comprising a DNAzyme-cleaved reaction for high sensitive uranyl ion (UO_2^{2+}) detection in natural water.³⁶ Fig. 4 presents the schematic representation of PNI sensors and corresponding SERS spectra for UO_2^{2+} detection (left panel). The magnified modification scheme of a PNI sensor with DNAzymes is shown on the right of the SERS spectra (right panel). The SERS detection was based on the UO_2^{2+} induces the cleavage of DNAzymes to released strands, then, Raman-active molecules and the PNI sensor capture the released strands with reporter-active molecules, giving strong SERS signal. The PNI sensor detected a low level of UO_2^{2+} as low as 1 pM with a wide dynamic range from 1 pM to 10 nM. Importantly, the PNI sensors exhibited high selectivity towards other metal ions (e.g., Cd^{2+} , Hg^{2+} , Pb^{2+} , Ca^{2+} , Mg^{2+} , Zn^{2+} , Cu^{2+} , Fe^{2+} , Co^{2+} , Ni^{2+} , and Th^{4+}) at 10 nM.³⁶

4. Applications of Au NWs Based SERS Platform in Biosensing

Sensitive, accurate, reproducible, and specific detections of biomolecules or biomarkers are very challenging and have utmost importance for clinical and diagnostics purposes in biomedical applications. Single-crystalline AuNWs-based SERS biosensors have received intense attention and developed significantly during last few decades. In this section, single-crystalline AuNWs-based SERS biosensors for biomolecular detections will be summarized.

A PNI sensor based on single-crystalline AuNWs on Au film (AuNWs/Au) was developed for the attomolar detection of biomarkers of prostate cancer, miR141 and miR375 which are released from living prostate cancer (PC) cells.³⁷ This sensor showed a magnificent ability to detect miRNAs with a wide dynamic range (from 100 aM to 100 pM) and an ultralow LOD as 100 aM. Moreover, single-base mismatches were discriminated by this PNI sensor, enabling the detection of extracellular miR141 and miR375 in the living PC cell lines (LNCaP and PC-3).³⁷ Therefore, the PNI sensor could be used as a strong diagnosis strategy to detect PC.

The Au particle-on-wire based SERS substrate was applied as a DNA biosensor (Fig. 5).³¹ The schematic illustrations of the Au particle-on-wire based SERS substrate is shown in Fig. 5(a). Fig. 5(b) and 5(c) show the modification scheme of the Au particle-on-wire based SERS sensor and SERS spectra from each of the four particle-on-wire system when the sample included two kinds of target DNAs (*E. faecium* and *S. maltophilia*). The EF of the sensor was determined to be 2.6×10^3 by monitoring the 1580 cm^{-1} band intensity of Cy5 as the concentration of target DNAs changed. Additionally, linear dynamic range and LOD were determined to be 10^{-11} – 10^{-8} M and 10 pM, respectively, corresponding to 300 amol (300×10^{-18} mole). To evaluate practical applicability, the system was employed for pathogen diagnosis using the target DNAs prepared by polymerase chain reaction (PCR) amplification of the genomic DNAs extracted from four reference pathogenic strains (*Enterococcus*

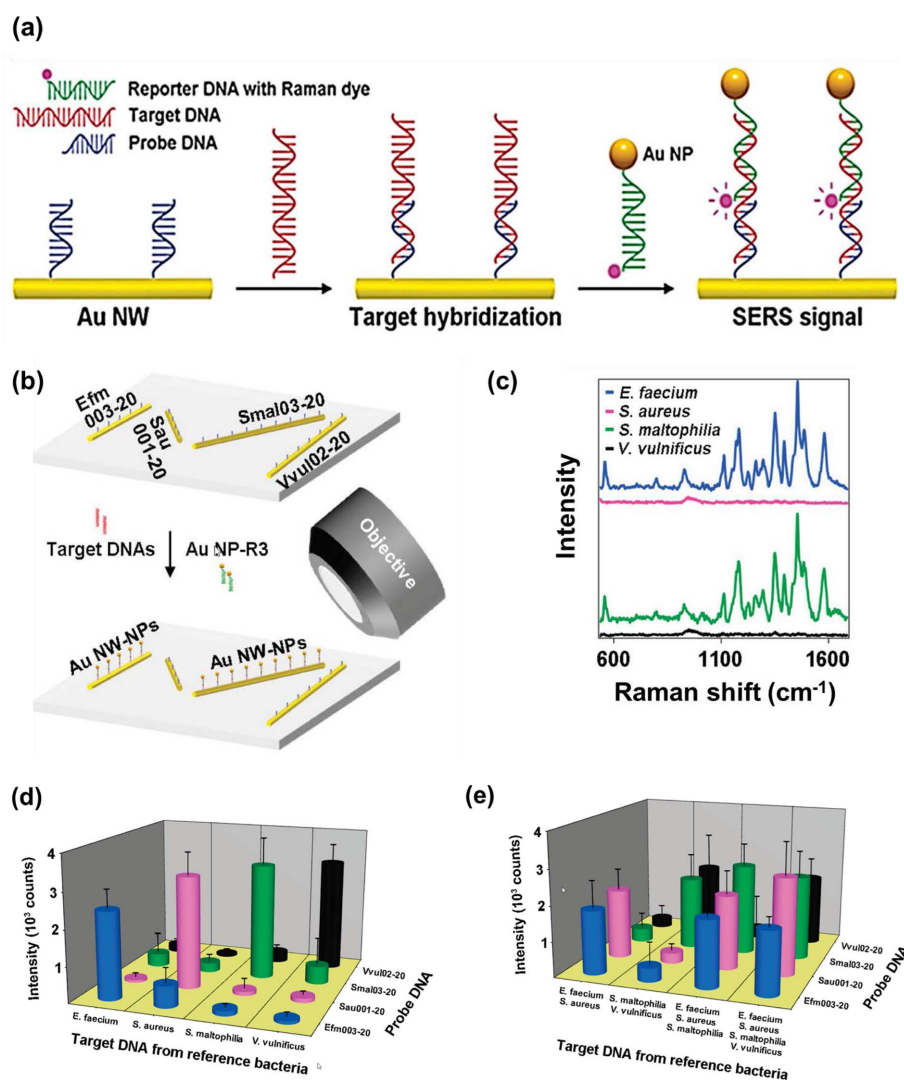


Fig. 5. (a) Schematic representation for the patterned multiplex pathogen DNA detection using a particle-on-wire SERS sensor.²³ (b) modification of the Au particle-on-wire SERS sensors, (c) SERS spectra from each of the four particle-on-wire system when the sample included two kinds of target DNAs (*E. faecium* and *S. maltophilia*), (d) Bar graph representation of the detection of only one kind of target DNA at 10^{-8} M concentration, (e) and two, three, and four kinds of target DNAs at concentrations of each 10^{-8} M). Copyright 2010 American Chemical Society.

faecium, *Staphylococcus aureus*, *Stenotrophomonas maltophilia*, and *Vibrio vulnificus*). Fig. 5(d) and 5(e) show the bar graph representation of the detection of only one kind of target DNA at 10^{-8} M and multiple kinds of target DNAs at 10^{-8} M each. The SERS PNI biosensors successfully detected various DNAs individually or unitedly at 100 nM, indicating the high potentiality of the Au particle-on-wire sensor for pathogen detections.³¹

Another AuNWs based PNI sensors for highly-specific and high sensitive (at zeptomole) detection of miRNAs was developed through bi-temperature hybridizations method (Fig. 6).³⁴ Fig. 6(a) shows the schematic representation of miRNA detection by PNI sensors working with bi-temperature hybridization. Fig. 6(b) and 6(c) show the SERS spectra of Cy5 measured from PNI sensors in the presence of perfectly matched miRNA and of single base mismatched

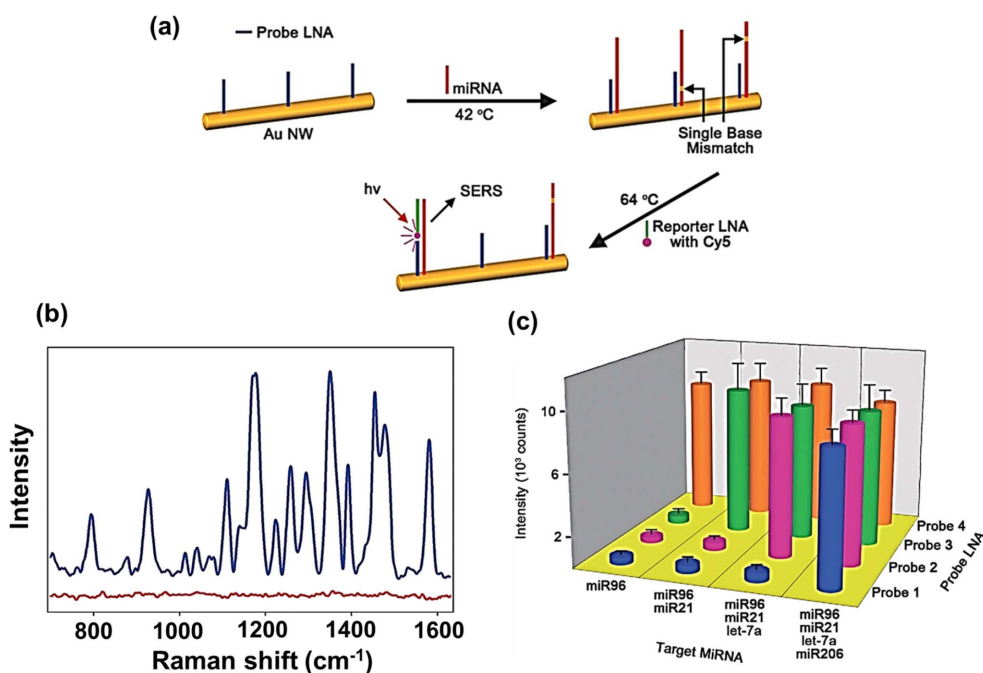


Fig. 6. (a) Schematic representation of miRNA detection by PNI sensors worked with bi-temperature hybridization method.²⁷ (b) SERS spectra of Cy5 measured from PNI sensors in the presence of perfectly matched miRNA (miR206; blue spectrum) and of single base mismatched miRNA (miR206 A; red spectrum), both in 100 pM concentrations, and (c) bar graph representation of the 1580 cm⁻¹ band intensities measured from each PNI sensor when the sample contains one, two, three, and four kinds of target miRNAs 100 pM concentration each. Copyright 2014 Wiley-VCH Verlag GmbH & Co. KGaA

miRNA and bar graph representation of the 1580 cm⁻¹ band intensities measured from each PNI sensor when the sample contains multiple kinds of target miRNAs, respectively. This method shows near-perfect accuracy of single nucleotide polymorphism (SNPs) and exhibits a wide dynamic range (100 aM–100 pM) and an ultralow LOD of 100 aM (50 zeptomole) without any amplification/labeling steps and chemical/enzymatic reactions. The multiplex sensing capability of this sensor was examined by detecting various miRNAs in the mixture of miRNA. The sensor was also applied to investigate the expression patterns of four miRNAs in human tissues including skeletal muscle and heart tissues. The resultant SERS signals show varying levels of miR206, let-7a, and miR21 in the total RNA extracts from human tissues with very low miR96 expression indicating the present PNI sensor has outstanding ability for multiplexed miRNA detection.³⁴ Using the

similar type of PNI sensor, an attomolar detection of miR141 and miR375 released from living PC cells was achieved.³⁷ This PNI sensor also exhibited an ultralow detection limit (100 aM) and a wide dynamic range (100 aM to 100 pM) for all target miRNAs. Additionally, the PNI sensor could discriminate perfectly the diverse single-base mismatches in the miRNAs and successfully detected the extracellular miR141 and miR375 released from living PC cell lines (LNCaP and PC-3), proving the excellent diagnostic ability of the sensor for PC.

In addition, a nanogap-rich AuNW SERS platform has been reported for the detection of telomerase activity in various cancer cells and tissues.³⁸ The substrate was constructed by depositing AuNPs on single-crystalline AuNWs, which provided highly reproducible SERS spectra. The EF of nanogap-rich AuNWs was determined to be 1.34×10^4 . The telomeric substrate (TS) primer-attached nanogap-rich AuNWs

successfully detected telomerase activity in various cancer cell lines (gastric and breast cancer) with a LOD of 0.2 cancer cells mL⁻¹ and RSD of 4.8% with the elongation of TS primers, folding into G-quadruplex structures, and intercalation of methylene blue,³⁸ demonstrating the excellent ability of the nanogap rich AuNW sensor for diagnosing gastric and breast cancer tissues accurately. The sensor could be applied for diagnosis of gastric and breast cancer with more accuracy compared to previously developed strategies.

5. Conclusions and Future Perspective

In this review, we have discussed the development of the AuNWs based SERS sensors for chemicals and biological molecules. The important issues are to make high SERS enhancement ability with high reproducibility, inexpensive, and easy sensor fabrication. Although the VP method is simple and easy to use, the use of high temperature in the synthesis of AuNWs is still relatively expensive, which need to minimize. Most of the work described here showed very high sensing ability in terms of EF value, but only few of them discussed the systematic analytical detection of analytes with specificity issue and real sample analysis. The further development of the AuNWs based SERS sensors and biosensors must be followed to validate and translate the current substrates to point-of-care devices for improving the quality of our life in detection of food contaminants, pollutants, biomolecules, and pathogens detection. It is expected that the AuNWs based SERS sensor and biosensors will be one of potential tools in routine environmental, food, medical, biochemical, and biological analyses in future.

Acknowledgements

R.A. and H.-J. L. contributed equally to this work. This work is supported by the National Research Foundation of Korea (NRF) grants funded by the Ministry of Science and ICT of Korea (MSIT) (NRF-2022R1C1C1005761 and RS-2023-00221237).

References

1. J. P. Camden, J. A. Dieringer, J. Zhao, and R. P. Van Duyne, *Acc. Chem. Res.*, **41**, 1653-1661 (2008). <https://doi.org/10.1021/ar800041s>
2. J. Langer, L. M. Liz-Marzan et al., *ACS Nano*, **14**, 28-117 (2020). <https://doi.org/10.1021/acsnano.9b04224>
3. B. Sharma, M. F. Cardial, S. L. Kleinman, N. G. Greeneltch, R. R. Frontiera, M. G. Blaber, G. C. Schatz, and R. P. Van Duyne, *MRS Bull.*, **38**, 615-624 (2013). <https://doi.org/10.1557/mrs.2013.161>
4. K. Kneipp, H. Kneipp, I. Itzkan, R. R. Dasari, and M.S. Feld, *Chem. Rev.*, **99**, 2957-2975 (1999). <https://doi.org/10.1021/cr980133r>
5. G. Braun, I. Pavel, A. R. Morrill, D. S. Seferos, G. C. Bazan, N. O. Reich, and M. Moskovits, *J. Am. Chem. Soc.*, **129**, 7760-7761 (2007). <https://doi.org/10.1021/ja072533e>
6. I. Yoon, T. Kang, W. Choi, J. Kim, Y. Yoo, S.-W. Joo, Q.-H. Park, H. Ihee, and B. Kim, *J. Am. Chem. Soc.*, **131**, 758-762 (2009). <https://doi.org/10.1021/ja807455s>
7. S. J. Lee, Z. Guan, H. Xu, and M. Moskovits, *J. Phys. Chem. C*, **111**, 17985-17988 (2007). <https://doi.org/10.1021/jp077422g>
8. M. Moskovits, *Rev. Mod. Phys.*, **57**(3), 783-826 (1985). <https://doi.org/10.1103/RevModPhys.57.783>
9. A. Sabur, M. Havel, and Y. J. Gogotsi, *J. Raman Spectrosc.*, **39**, 61-67 (2008). <https://doi.org/10.1002/jrs.1814>
10. T. Kang, I. Yoon, K.-S. Jeon, W. Choi, Y. Lee, K. Seo, Y. Yoo, Q. Park, H. Ihee, Y. D. Suh, and B. Kim, *J. Phys. Chem. C*, **113**, 7492-7496 (2009). <https://doi.org/10.1021/jp809391c>
11. E. C. Le Ru and P. G. Etchegoin, *Chem. Phys. Lett.*, **423**(1-3), 63-66 (2006). <https://doi.org/10.1016/j.cplett.2006.03.042>
12. E. C. Le Ru, M. Meyer, and P. G. Etchegoin, *J. Phys. Chem. C*, **111**, 13794-13803 (2007). <https://doi.org/10.1021/jp0687908>
13. M. E. Stewart, C. R. Anderton, L. B. Thompson, J. Maria, S. K. Gray, J. A. Rogers, and R. G. Nuzzo, *Chem. Rev.*, **108**, 494-521 (2008). <https://doi.org/10.1021/cr068126n>
14. A. G. Brolo, E. Aretander, R. Gordon, B. Leathem, and K. L. Kavanagh, *Nano Lett.*, **4**, 2015-2018 (2004). <https://doi.org/10.1021/nl048818w>
15. Q. Yu, Y. Wu, T. Kang, and J. Choo, *Bull. Kor. Chem. Soc.*,

- 42, 1699-1705 (2021). <https://doi.org/10.1002/bkcs.12418>
16. H. J. Park, S. C. Yang, and J. Choo, *Bull. Kor. Chem. Soc.*, **37**, 2019-2024 (2016). <https://doi.org/10.1002/bkcs.11021>
 17. L. Chen, Y. Sa, X. Wang, B. Zhao, and Y. M. Jung, *Bull. Kor. Chem. Soc.*, **36**, 930-935 (2015). <https://doi.org/10.1002/bkcs.10174>
 18. H. Dang, Y. Joung, C. Jeong, C. S. Jeon, S. H. Pyun, S.-G. Park, and J. Choo, *Bull. Kor. Chem. Soc.*, **44**, 441-448 (2023). <https://doi.org/10.1002/bkcs.12679>
 19. W.-S. Yoon, J.-H. Im, and J.-H. Kim, *Anal. Sci. Technol.*, **8**, 699-705 (1995).
 20. K. C. See, J. P. Spicer, J. Brupbacher, D. Zhang, and T. J. Vargo, *J. Phys. Chem. B*, **109**, 2693-2698 (2005). <https://doi.org/10.1021/jp046687h>
 21. Q. Dai, J. Huang, X. Qiu, X. Chen, and Y. Li, *ACS Appl. Nano Mater.*, **7**, 6369-6379 (2024). <https://doi.org/10.1021/acsnm.4c00034>
 22. Y. Jia, L. Zhang, L. Song, L. Dai, X. Lu, Y. Huang, J. Zhang, Z. Guo, and T. Chen, *Langmuir*, **33**, 13376-13383 (2017). <https://doi.org/10.1021/acs.langmuir.7b03261>
 23. Y. Zhu, X. Qiu, X. Chen, M. Huang, and Y. Li, *Talanta*, **249**, 123675 (1-7) (2022). <https://doi.org/10.1016/j.talanta.2022.123675>
 24. Y. Tian, X. Li, F. Wang, C. Gu, Z. Zhao, H. Si, and T. Jiang, *J. Hazard. Mater.*, **403**, 124009 (1-14) (2021). <https://doi.org/10.1016/j.jhazmat.2020.124009>
 25. T. Jiang, X. Wang, J. Zhou, and H. Jin, *Sens. Actuators B: Chem.*, **258**, 105-114 (2018). <https://doi.org/10.1016/j.snb.2017.11.084>
 26. K. Li, Y. Yang, C. Xu, Y. Ye, L. Huang, L. Sun, Y. Cai, W. Zhou, Y. Ge, Yang Li, Q. Zhang, Y. Wang, and X. Liu, *Sens. Actuators B: Chem.*, **380**, 133381 (1-9) (2023). <https://doi.org/10.1016/j.snb.2023.133381>
 27. C. Wang, J. Han, D. Xue, C. Gu, S. Zeng, J. Jiang, T. Jiang, X. Li, and K. Wu, *Spectrochem. Acta A Mol. Biomol. Spectrosc.*, **305**, 123445 (1-10) (2024). <https://doi.org/10.1016/j.saa.2023.123445>
 28. M. Kang, H. Lee, T. Kang, and B. Kim, *J. Mater. Sci. Technol.*, **31**, 573-580 (2015). <https://doi.org/10.1016/j.jmst.2015.01.007>
 29. J. W. Jeong, M. M. P. Arnob, K.-M. Baek, S.Y. Lee, W.-C. Shih, and Y. S. Jung, *Adv. Mater.*, **28**, 8695-8704 (2016). <https://doi.org/10.1002/adma.201602603>
 30. P. Li, Y. Li, Z.-K. Zhou, S. Tang, X.-F. Yu, S. Xiao, Z. Wu, Q. Xiao, Y. Zhao, H. Wang, and P. K. Chu, *Adv. Mater.*, **28**, 2511-2517 (2016). <https://doi.org/10.1002/adma.201505617>
 31. T. Kang, S. M. Yoo, I. Yoon, S. Y. Lee, and B. Kim, *Nano Lett.*, **10**, 1189-1193 (2010). <https://doi.org/10.1021/nl1000086>
 32. Y. Yoo, K. Seo, S. Han, K. S. K. Varadwaj, H. Y. Kim, J. H. Ryu, H. M. Lee, H. M. J. P. Ahn, H. Ihee, and B. Kim, *Nano Lett.*, **10**, 432-438 (2010). <https://doi.org/10.1021/nl903002x>
 33. T. Kang, S. M. Yoo, M. Kang, H. Lee, H. Kim, S. Y. Lee, and B. Kim, *Lab Chip.*, **12**, 3077-3081 (2012). <https://doi.org/10.1039/c2lc40185a>
 34. T. Kang, H. Kim, J. M. Lee, H. Lee, Y.-S. Choi, G. Kang, M.-K. Seo, B. H. Chung, Y. Jung, and B. Kim, *Small*, **10**, 4200-4206 (2014). <https://doi.org/10.1002/smll.201400164>
 35. H. Kim, M.-L. Seol, D.-I. Lee, J. Lee I.-S. Kang, H. Lee, T. Kang, Y. K. Choi, and B. Kim, *Nanoscale*, **8**, 8878-8886 (2016). <https://doi.org/10.1039/c6nr00092d>
 36. R. Gwak, H. Kim, S. M. Yoo, S. Y. Lee, G.-J. Lee, M.-K. Lee, C.-K. Rhee, T. Kang, and B. Kim, *Sci. Rep.*, **6**, 19646 (1-6) (2016). <https://doi.org/10.1038/srep19646>
 37. S. Yang, H. Kim, K. J. Lee, S. G. Hwang, E.-K. Lim, J. Jung, T. J. Lee, H.-S. Park, T. Kang, and B. Kim, *Nanoscale*, **9**, 17387-17395 (2017). <https://doi.org/10.1039/c7nr04386d>
 38. G. Eom, H. Kim, A. Hwang, H.-Y. Son, Y. Choi, J. Moon, D. Kim, M. Lee E.-K. Lim, J. Jeong, Y.-M. Huh, M.-K. Seo, T. Kang, and B. Kim, *Adv. Funct. Mater.*, **27**, 1701832 (1-10) (2017). <https://doi.org/10.1002/adfm.201701832>

Authors' Positions

Rashida Akter	: Postdoctoral Scholar
Hyuck jin Lee	: Associate Professor
Toeun Kim	: Graduate Student
Jin Woo Choi	: Assistant Professor
Hongki Kim	: Assistant Professor